International Journal of Concrete Structures and Materials

RESEARCH Open Access

Analytical Model for Seismic Performance of Hollow RC Bridge Piers Considering Elongation Reduction in Reinforcement Deteriorated by Aging and Other Factors

Tae-Hoon Kim[1*], Ick-Hyun Kim[2] and Hyun Mock Shin[3]

Abstract

This study presents an analytical technique for understanding the seismic behavior and evaluating the seismic performance of hollow RC bridge piers deteriorated by aging and other factors. Deterioration caused by de-icing agents and carbonation has reduced the lifespan of bridge structures, thus necessitating frequent maintenance and increasing economic and social costs. A validated nonlinear finite element analysis program RCAHEST (Reinforced Concrete Analysis in Higher Evaluation System Technology) was enhanced with a deterioration model and an extended damage index that incorporates elongation reduction in reinforcing bars. The modified nonlinear material model accounts for the reduction of cross-sectional area of reinforcement and the change of bond strength at the concrete-to-steel interface caused by corrosion. Extended damage indices considering elongation reduction of reinforcing bars aim to provide a means of quantifying numerically the damage in deteriorated hollow RC bridge piers under earthquake loading. This approach allowed for a reliable parametric study of deteriorated hollow RC bridge piers, resulting in accurate predictions of performance degradation and the reversal phenomenon of the damage index due to drift ratios. The proposed nonlinear analysis method was validated to properly account for key design variables, including corrosion level, yield strength and ultimate strength of the reinforcing bars, and compressive strength of the concrete. Additionally, the newly extended damage index, which incorporates both the deterioration model and elongation reduction in reinforcing bars affecting behavior, effectively evaluates seismic performance.

Keywords Seismic performance, Hollow RC bridge piers, Deteriorated, Damage index, Elongation reduction

1 Introduction

Recent earthquakes in different countries have caused damage to infrastructure, including bridge structures, thus highlighting an urgent need for research on accurately evaluating and enhancing the seismic performance of these public structures. In addition, unexpected structural behavior mechanisms are occurring due to deterioration, such as aging, leading to problems like performance degradation (Ueda & Takewaka, 2007; Apostolopoulos & Papadakis, 2008; Apostolopoulos et al., 2013; Biondini et al., 2014; Xu et al., 2021).

Hollow bridge piers, widely used in bridge structures, are lighter than solid bridge piers, resulting in a reduced

Journal information: ISSN 1976-0485 / eISSN 2234-1315.

*Correspondence:
Tae-Hoon Kim
thkim@krri.re.kr
[1] Advanced Railroad Civil Engineering Division, Korea Railroad Research Institute, 176, Cheoldobangmulgwan-ro, Uiwang-si 16105, Gyeonggi-do, Korea
[2] Department of Civil and Environmental Engineering, University of Ulsan, 93, Daehak-ro, Ulsan-si 44610, Korea
[3] School of Civil, Architectural Engineering, and Landscape Architecture, Sungkyunkwan University, Seobo-ro, Suwon-si 206616419, Gyeonggi-do, Korea

load on the foundation structure and lower inertial forces during earthquakes, thus making hollow bridge piers relatively advantageous compared to solid bridge piers (Yeh et al., 2001; Sun & Kim, 2009; Lignola et al., 2012; Kim et al., 2019). Additionally, they are commonly used in the design and construction of railway bridges due to their favorable mechanical behavior, such as a higher second moment of area. Furthermore, studies are continuously being conducted to investigate the seismic behavior of hollow bridge piers (Cardone et al., 2013; Cassese et al., 2020; Kim et al., 2014; Lee et al., 2017).

The seismic performance evaluation technique based on damage indices has been validated for appropriately assessing the seismic performance of both solid and hollow RC bridge piers subjected to cyclic loads, such as earthquake loads. Additionally, nonlinear finite element analysis can help evaluate the actual behavior and seismic performance of multi-degree-of-freedom structures, such as reinforced concrete (RC) bridges (Kim, 2019, 2022; Kim et al., 2005, 2007).

In recent years, deterioration caused by de-icing agents and carbonation has reduced the lifespan of bridge structures, thus necessitating frequent maintenance and increasing economic and social costs (El-Joukhadar et al., 2023). Corrosion resulting from this deterioration reduces the cross-sectional areas of reinforcing bars and degrades bonding performance due to concrete cover cracks and corrosion products. This degradation in bonding performance significantly affects the seismic performance and structural behavior of RC, such as tensile hardening behavior (Ahmadi et al., 2021; Crespi et al., 2022; Ghosh & Padgett, 2012; Pantazopoulou & Papoulia, 2001; Rajput & Sharma, 2018; Rinaldi et al., 2022; Stewart & Al-Harthy, 2008; Toongoenthong & Maekawa, 2005; Zucca et al., 2023). Additionally, the loss due to corrosion is more pronounced when reinforcing bars are embedded in concrete because chloride-induced corrosion creates active and passive areas, known as the macro-cell effect, in the metal (Apostolopoulos et al., 2013).

The deterioration of concrete structures, as described above, results in substantial economic costs for maintenance and reinforcement. According to a study by Ueda & Takewaka (2007), maintenance and repair costs can amount to as much as 50% of the investment in civil engineering construction in some European countries.

In the failure of RC bridge piers due to the fracture of reinforcing bars, i.e., the focus of this study, the fracture of longitudinal reinforcing bars is governed by the low-cycle fatigue behavior of the reinforcement. The fracture of transverse reinforcing bars is influenced by the axial force of the bridge pier and the strain in the transverse reinforcement, which depends on the amount of transverse reinforcing bars. Additionally, elongation, a fundamental mechanical property of reinforcing bars, has a significant impact on seismic performance (Lee et al., 2011). Therefore, the nonlinear program RCAHEST (Reinforced Concrete Analysis in Higher Evaluation System Technology) (Kim, 2019, 2022, 2023; Kim et al., 2005, 2007, 2019)—modified to account for uncertainties such as uniform corrosion, pitting corrosion of reinforcing bars, and the reduction in bond strength between concrete and reinforcement—was further extended to consider the elongation reduction of newly deteriorated reinforcing bars. The extended RCAHEST program was then used to evaluate the behavior and seismic performance of RC hollow bridge piers that have deteriorated due to aging and other factors. This study also extended the seismic performance evaluation technique using damage indices to assess hollow RC bridge piers that have deteriorated due to aging and other factors. The validity of this technique was verified using quasi-static experimental results from previous studies on hollow RC bridge pier specimens.

2 Consideration of Elongation Reduction and Deterioration of Reinforcing Bars Due to Aging and Other Factors

2.1 Elongation Reduction of Deteriorated Reinforcing Bars

The numerical simulation of hollow RC bridge piers deteriorated due to aging and other factors is highly complex due to various uncertainties. Therefore, to evaluate long-term seismic performance, it is essential to develop an analytical technique that can overcome the limitations of experimental methods. Previous studies (Kim, 2022, 2023) have investigated the impacts of corrosion on structural performance, including concrete cracks, reduction of the cross-sectional area of reinforcing bars, decreased bond strength between reinforcing bars and concrete, and the degradation of mechanical properties of corroded reinforcing bars. Additionally, related deterioration models were developed and applied.

In this study, the reduction in the elongation of deteriorated reinforcing bars, which significantly impacts seismic performance, was newly considered. Generally, as the corrosion level of reinforcing bars increases, the nominal yield strength and nominal elastic modulus decrease, and the corrosion level is highly correlated with the mechanical properties of reinforcing bars (Lee & Cho, 2009; Lee et al., 2011). Furthermore, after tensile testing, it was found that failure often initiates from localized corrosion, such as pitting, leading to brittle failure with low strength and low elongation. The elongation of reinforcing bars must be considered as it significantly affects the ductility of RC members.

Elongation is determined by conducting a monotonic tensile test on reinforcing bars and is calculated using Eq. (1).

$$\delta = \frac{l - l_0}{l} \tag{1}$$

Here, δ denotes the elongation, l_0 represents the gauge length, and l is the length between the gauge points measured after fracture.

Final elongation is determined by testing the specimen under a tensile load and measuring the elongation after the reinforcing bar fractures. Additionally, the surface of the specimen is marked before conducting the tensile test to define the gauge length and verify the elongation of the reinforcing bar.

When measuring the elongation of reinforcing bars that have deteriorated due to aging and other factors, fracture occurs after necking develops at a length smaller than the measured elongation length once the ultimate strength is reached. El-Joukhadar et al. (2023) proposed Eq. (2) for the residual maximum elongation of corroded reinforcing bars based on a regression analysis of experimental data (see Fig. 1).

$$\varepsilon_{u,res} = \varepsilon_u \cdot e^{-0.057x} \tag{2}$$

Here, $\varepsilon_{u,res}$ represents the ultimate elongation, ε_u denotes the ultimate strain, and x is the average mass reduction of the reinforcing bars.

2.2 Nonlinear Material Model Considering Deterioration

In this study, the deterioration model (Kim, 2022, 2023)—developed to represent the reduction in cross-sectional area due to the corrosion of reinforcing bars, degradation in bond strength and ductility, and reduced strength due to concrete cracks—was modified to suit the structural behavior of hollow RC bridge piers deteriorated by aging and other factors. Additionally, the elongation reduction of deteriorated reinforcing bars, as discussed in the previous section, was incorporated. This process can be summarized as follows:

The equation proposed by Bhargava et al. (Bhargava et al., 2007), based on the pullout results of RC corrosion test specimens, was applied to represent nonlinear behavioral characteristics such as bond strength degradation due to the corrosion of reinforcing bars. A realistic analytical model of bond strength degradation is determined using fracture mechanics combining the action of adhesion, confining pressure and corrosion pressure at steel concrete interface (Nepal et al., 2013).

Here, the bond strength degradation was calculated as the ratio between the bond strength of uncorroded reinforcing bars and that of corroded reinforcing bars, according to the level of corrosion.

$$R_{dhc} = 1.0 \text{ for } C_{dhc} \leq 1.5\% \tag{3}$$

$$R_{dhc} = 1.192e^{-0.117C_{dhc}} \text{ for } C_{dhc} > 1.5\% \tag{4}$$

$$C_{dhc} = \frac{\Delta W_{dhc}}{W_{dhc}} \times 100 \tag{5}$$

Here, R_{dhc} represents the ratio between the bond strength of uncorroded reinforcing bars and that of corroded reinforcing bars, C_{dhc} denotes the corrosion level, ΔW_{dhc} is the average mass reduction of the reinforcing bars, and W_{dhc} denotes the mass of uncorroded reinforcing bars.

Moreover, the reduction in the cross-sectional area of the corroded reinforcing bars was represented using the following equation.

$$A_{sdhc} = A_{shc}(1 - 0.01C_{dhc}) \tag{6}$$

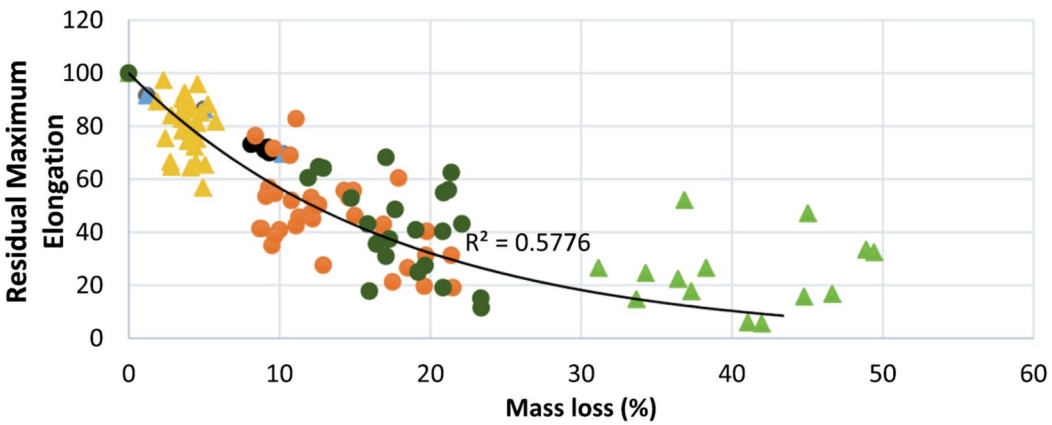

Fig. 1 Residual maximum elongation of corroded reinforcement vs mass loss (El-Joukhadar et al. (2023))

Here, A_{sdhc} denotes the cross-sectional area of the corroded reinforcing bars, and A_{shc} represents the cross-sectional area of the uncorroded reinforcing bars.

3 Nonlinear Finite Element Analysis Program RCAHEST and Extended Damage Indices

3.1 Nonlinear Finite Element Analysis Program RCAHEST

In this study, a model that accounts for the reduction in elongation and deterioration of reinforcing bars due to aging and other factors, as described in Sect. 2, was added to the nonlinear program RCAHEST (Reinforced Concrete Analysis in Higher Evaluation System Technology) (Kim, 2019, 2022, 2023; Kim et al., 2005, 2007, 2019) developed to date. RCAHEST incorporates plane stress elements, joint elements, and interface elements—all developed by the authors—into the Finite Element Analysis Program (FEAP) developed by Professor Taylor at UC Berkeley (Taylor, 2000). The existing RC material model serves as the nonlinear material model in the RCAHEST program.

The non-orthogonal fixed crack model applied in this study compensates for the drawback of the orthogonal fixed crack model, which overestimates concrete stiffness by restricting secondary cracks from forming orthogonally to primary cracks (Kim et al., 2005). This allows for a more realistic evaluation of concrete stiffness.

Based on these cracks, the mechanical behavior of concrete before cracking is represented by the basic concept of the elastic–plastic failure model for a biaxial stress state, while nonlinearity becomes significant after cracks occur. For post-cracking nonlinearity, the tension stiffening model, compression stiffness model, and shear transfer model were applied according to the orthotropic assumption of RC elements. As shown in Fig. 2, the tension stiffening model represents the tensile stress carried by the concrete perpendicular to the cracks; the compression stiffness model accounts for the degradation of compressive stiffness parallel to the cracks; and the shear transfer model addresses the shear transfer effect of the cracked surface.

The post-yield behavior of reinforcing bars embedded in concrete must be considered alongside the characteristics of the reinforcing bars and the bond effect between the concrete and the reinforcing bars. Stress does not increase due to the yielding of reinforcing bars in the cracked area. However, the internal stress within the reinforcing bars increases, leading to a rise in the average stress of the bars. As a result, the yield plateau phenomenon, typically observed in the stress–strain relationship of the reinforcing bars alone, is not seen. This post-yield behavior of reinforcing bars in the envelope region is represented by the bilinear model proposed by the authors, as shown in Fig. 3.

Transverse confinement reinforcement increases the ultimate strength and ultimate strain of concrete. As a result, confined concrete exhibits superior resilience and ductility compared to unconfined concrete when subjected to earthquake loads (Mander et al., 1988). In this study, a coefficient that adjusts the transverse confinement effect according to the hollow dimension

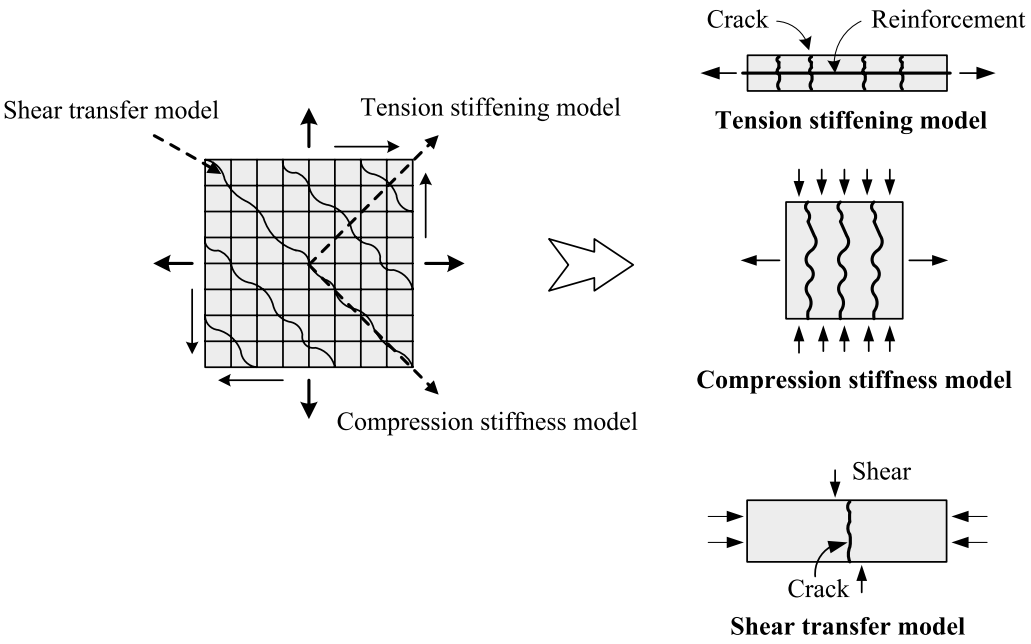

Fig. 2 Cracked concrete model

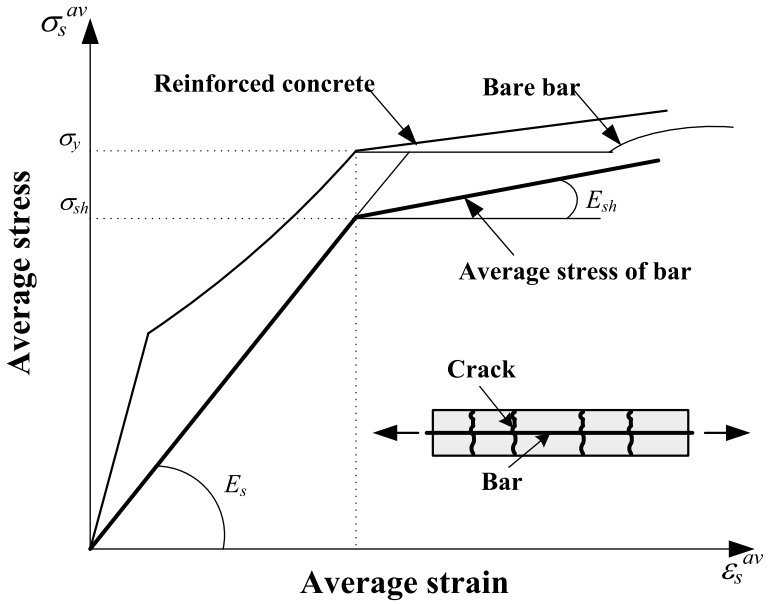

Fig. 3 Reinforcing bar model in concrete

ratio was incorporated into the model proposed by the authors (Kim, 2019, 2022; Kim et al., 2005, 2007, 2019). This model accounts for the amount of transverse confinement reinforcement, longitudinal reinforcement, yield strength, and the arrangement of reinforcing bars, regardless of the cross-sectional shape of the concrete. Additionally, the mechanical properties of concrete experiencing compressive failure were considered. It was assumed that when compressive failure occurs in the concrete surrounding the reinforcing bars, the reinforcing bars also buckle. In this case, the stress in the reinforcing bars was considered to be 20% of the stress obtained without accounting for buckling, consistent with compressive failure in concrete (Kim, 2019, 2022; Kim et al., 2005, 2007, 2019).

Moreover, local discontinuous displacements, such as anchorage slip of reinforcing bars, penetration of the joint surface, and sliding of the joint surface, occur in the foundation of hollow RC bridge piers due to a sudden change in cross-sectional stiffness at the joints between members of different thicknesses. These local discontinuous displacements were addressed by applying the interface elements developed by the authors (Kim, 2019, 2022; Kim et al., 2005, 2007, 2019).

3.2 Extended Damage Indices

The damage index developed in previous studies (Kim, 2019, 2022, 2023; Kim et al., 2005, 2007, 2019) is an innovative method for evaluating the damage level of a structure, as illustrated in Fig. 4. The damage index quantitatively represents the extent of damage to the structure under load and reflects the performance characteristics of the entire structure. Previous studies developed a technique to calculate the damage index directly from the strain at the Gauss integration points of each element, obtained during nonlinear finite element analysis. To evaluate the seismic performance of hollow RC bridge piers deteriorated by aging and other factors, this study further extended the technique to include the deterioration model and the reduction in elongation of reinforcing bars, which influence the behavior.

A reliable nonlinear finite element analysis accounts for stiffness degradation, strength reduction, fatigue damage, and energy dissipation in hysteresis curves. Therefore, the strain at the Gauss integration points of each element provides sufficient information for evaluating the level of damage to the structure.

The performance level can be defined as the damage state determined by the limit state and is obtained by calculating the damage indices $DI_{compressive}$ and $DI_{tensile}$ based on the ultimate strain of concrete and reinforcing bars derived from finite element analysis. As shown in Fig. 4, the failure criteria can be classified into concrete compressive failure, shear failure, and tensile failure of reinforcing bars. The following equations represent the damage indices extended through this study:

$$DI_{compressive} = 1 - \Phi_c \left(\frac{2\varepsilon_{cu} - \varepsilon_{cs}}{2\varepsilon_{cu}} \right)^2 \tag{7}$$

$$DI_{tensile} = 1.20 \left(\frac{\varepsilon_{ts}}{2\Phi_r \Phi_e \varepsilon_{tu}} \right)^{0.67} \tag{8}$$

Performance level	Service	Repair	Damage	
			State	Index
Fully operational	Fully service	Limited epoxy injection	Hairline cracks	≤0.1
Delayed operational	Limited service	Epoxy injection, Concrete patching	Open cracks, Concrete spalling	≤0.4
Stability	Not useable	Replacement of damaged section	Bar buckling/Fracture, Core crushing	≤0.75

Material	Type of failure	Failure criterion (ε_{cu} or ε_{tu})	Extended dmage index ($DI_{compressive}$ or $DI_{tensile}$)
Concrete	Compressive and shear	$0.004+\frac{1.4\rho_s f_{yh}\varepsilon_{sm}}{f'_{cc}}$	$1-\Phi_c\left(\frac{2\varepsilon_{cu}-\varepsilon_{cs}}{2\varepsilon_{cu}}\right)^2$
Steel	Tensile	0.15	$1.20\left(\frac{\varepsilon_{ts}}{2\Phi_r\Phi_e\varepsilon_{tu}}\right)^{0.67}$

Fig. 4 Performance level assessment using an extended damage index

Here, $DI_{compressive}$ and $DI_{tensile}$ denote the compressive and tensile damage indices, respectively, while Φ_c and Φ_r represent the fatigue parameters for concrete and reinforcing bars, respectively. Additionally, ε_{cu} and ε_{tu} are the failure criteria based on the ultimate strains of concrete and reinforcing bars, respectively, whereas ε_{cs} and ε_{ts} denote the compressive and tensile strains at the analysis phase, respectively. Φ_e is the elongation reduction coefficient for reinforcing bars that have deteriorated due to aging and other factors.

A damage index of 0.0 indicates no damage, and a damage index of 1.0 indicates failure. A damage index of 0.75 denotes the point of failure. A modified damage index of 0.1 represents a state before the yielding of reinforcing bars, with slight flexural cracks, indicating a fully operational level. A damage index of 0.4 indicates that the reinforcing bars have yielded and there are significant flexural or shear cracks, resulting in spalling of the concrete cover. This damage index signifies an operational level. Furthermore, a damage index of 0.75 represents a state where reinforcing bars have begun to fracture, indicating a collapse prevention level.

4 Numerical Examples

4.1 Hollow RC Bridge Pier Specimens

Reliable experimental results from previous studies (Kim et al., 2014, 2019) were selected as numerical examples to validate the proposed numerical analysis method and to simulate mechanical behavior, such as the elongation reduction of deteriorated reinforcing bars.

The test specimens C-L and CC-80 from these studies (Kim et al., 2014, 2019) were used as hollow RC bridge pier specimens for the numerical example. Table 1 presents the material properties of these test specimens. For this study, the test specimens were designated HC-D1 and HC-D2, with details of the experiment shown in Fig. 5. The specimens were designed according to the Highway Bridge Design Standard (Ministry of Land, Infrastructure and Transport, 2015) and AASHTO LRFD (AASHTO, 2012), with the amount of transverse confinement reinforcement calculated based on a solid cross-section and considering only the exterior transverse reinforcement.

The outer diameter of the hollow RC bridge pier specimens is 1400 mm, with inner diameters of 980 mm and 1,050 mm, respectively. Thus, the hollow dimension ratios (inner diameter/outer diameter) are 0.70 and 0.75. The height of the bridge pier specimens is 4,900 mm, resulting in an aspect ratio of 3.5, which induces flexural failure behavior (Kolozvari et al., 2018).

The hollow RC pier specimens were consistently subjected to an axial force equivalent to 10% of the cross-sectional axial strength (see Fig. 6). To ensure that the axial force remained constant throughout the experiment, a device equipped with a hydraulic pump was used. Lateral loads were applied using a 3500 kN actuator, and the drift ratio was incrementally increased to 0.25%, 0.50%, 1.00%, 1.50%, 2.00%, 2.50%, 3.00%, 3.50%, 4.00%, 4.50%, and 5.00%. Each drift ratio was tested for two cycles. The number of displacement-controlled loads was chosen to investigate variations in seismic response characteristics for the same amplitude, changes in energy dissipation capacity, and the effect on strength degradation after reaching the maximum load-carrying capacity during seismic behavior.

To analyze the seismic behavior of the hollow RC bridge pier specimens, load measurements were taken using a load cell embedded in the actuator, while lateral displacements were measured with a linear variable differential transformer (LVDT). One LVDT was installed at the foundation to monitor its movement, and two LVDTs were positioned at the lateral loading point.

The quasi-static experimental results for these hollow RC bridge pier specimens are detailed in Kim et al. (2014) and Kim et al. (2019). The design values for load-bearing capacity, ductility, and energy dissipation capacity were well–satisfied. The analytical and experimental results indicated that stiffness, strength, and damage progression are influenced by the hollow dimension ratios (inner diameter/outer diameter), the amount and arrangement of lateral reinforcement, longitudinal steel percentage and the axial load ratio. Also, these parameters affected the location of the neutral axis and failure mode at failure. These factors should be considered in design and construction.

The HC-D1 specimen demonstrated a load-bearing capacity of up to 120% of the design load and met the required ductility of the bridge pier while exhibiting stable energy dissipation capacity. Similarly, the HC-D2 specimen achieved a load-bearing capacity of up to 145% of the design load, satisfied the required ductility, and showed stable energy dissipation capacity. The experimental results revealed that after horizontal cracks developed, concrete cover spalling and detachment occurred, leading to the buckling of the longitudinal reinforcing bars. As buckling progressed, internal concrete damage ensued, eventually resulting in the fracture of the longitudinal reinforcing bars. This fracture significantly impacted the stiffness and strength of the hollow RC bridge pier system.

4.2 Interpretation and Analysis of Experimental Results

In this study, nonlinear finite element analysis was conducted by partitioning the elements, as shown in Fig. 7.

Table 1 Properties of hollow RC bridge pier specimen

Specimen		HC-D1	HC-D2
Cylinder concrete strength (MPa)		22.0	28.1
Longitudinal reinforcement (D19)	ρ_l(%)	1.3	1.5
	f_{yl}(MPa)	376.0	408.3
Transverse reinforcement (D13)	Ratio (Compared to code)	Outer 0.0047 (49%), Inner 0.0047 (49%)	Outer 0.0047 (49%), Inner 0.0047 (49%)
	Space (mm)	Outer @80, Inner @80	Outer @80, Inner @80
	f_{yt}(MPa)	343.0	405.7
Cross-tie (D13)	Space (mm)	18@80	18@80
	f_{yt}(MPa)	343.0	405.7
Axial force ratio	$\frac{P}{f_{ck}A_g}$	0.1	0.1

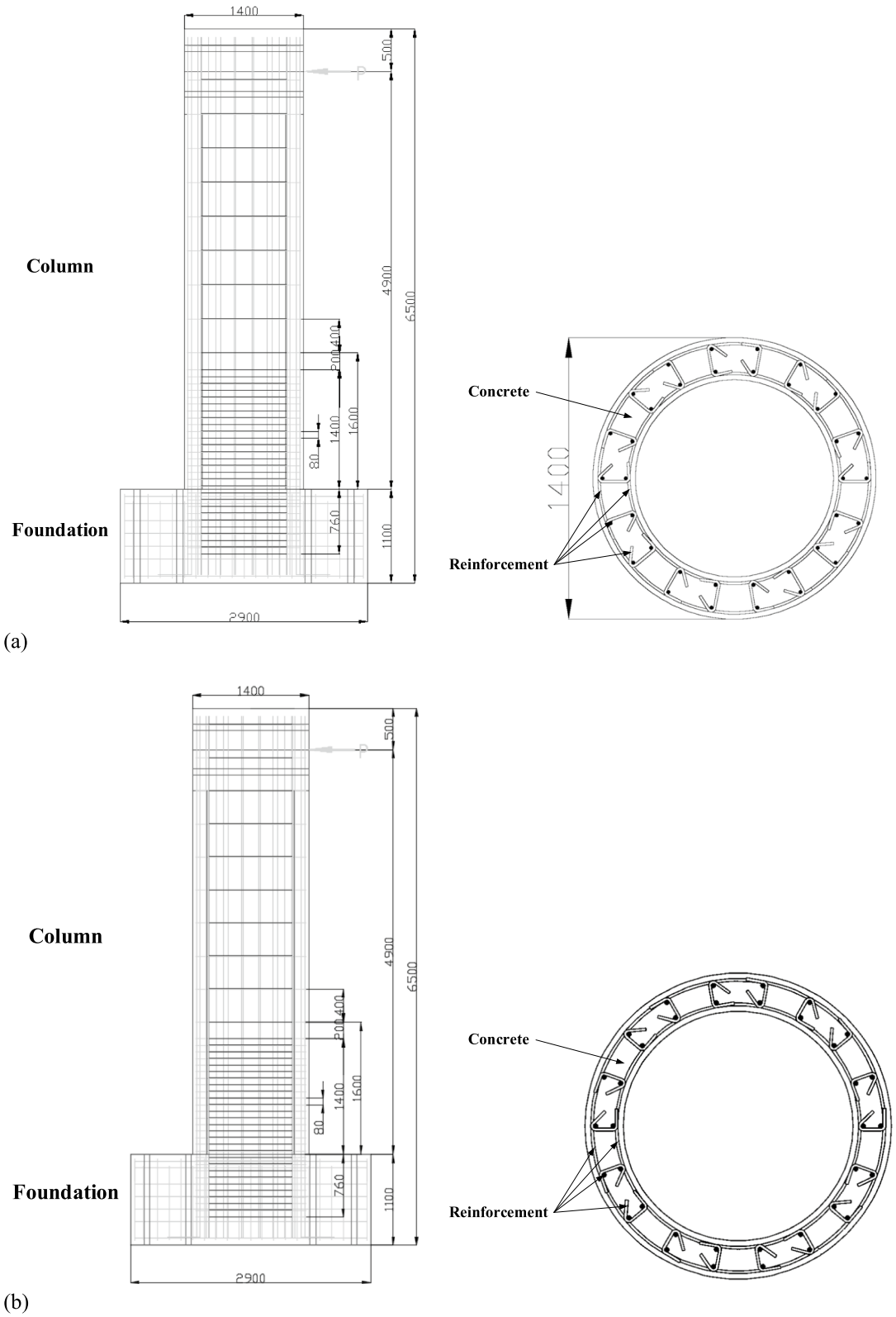

Fig. 5 Hollow RC bridge pier specimen (Unit: mm): **a** HC-D1 and **b** HC-D2

Fig. 6 Details of test setup

For the analysis of the hollow RC bridge pier specimens, an equivalent transformed cross-section was utilized (Fig. 7a, b) and a two-dimensional plane stress element was applied (Fig. 7c).

For rectangular sections, equivalent strips are calculated. After the internal forces are calculated, the equilibrium is checked. In this transformation of a circular section to a rectangular section, a section with minimum error was selected through iterative calculations concerning the moment of inertia for the sectional and area of concrete and reinforcements, to ensure that the behavior was similar to the actual behavior of the hollow RC bridge piers. Local discontinuous displacements—such as anchorage slip of reinforcing bars, joint surface sliding, and joint surface penetration—occurred in the foundation of each hollow RC bridge pier specimen due to abrupt changes in cross-sectional stiffness at joints between members with varying thicknesses. These displacements were simulated using interface elements, based on the discrete crack concept and assume that stress occurs only perpendicular to and parallel with the elements. Therefore, the nonlinear material model of RC described in Sect. 3.1 was applied accordingly (Kim et al., 2005, 2007).

The results of the nonlinear finite element analysis using the proposed analytical model, along with the experimental load–displacement relationships, are shown in Fig. 8. The maximum load, hysteresis curve, and post-failure behavior are in agreement.

The experimental hysteretic curves also shown in Fig. 8 exhibit asymmetry. It was found that the main reasons were slip between base plate and column foundation, and initial axial load eccentricity. However, the analytical hysteretic curves exhibit symmetry.

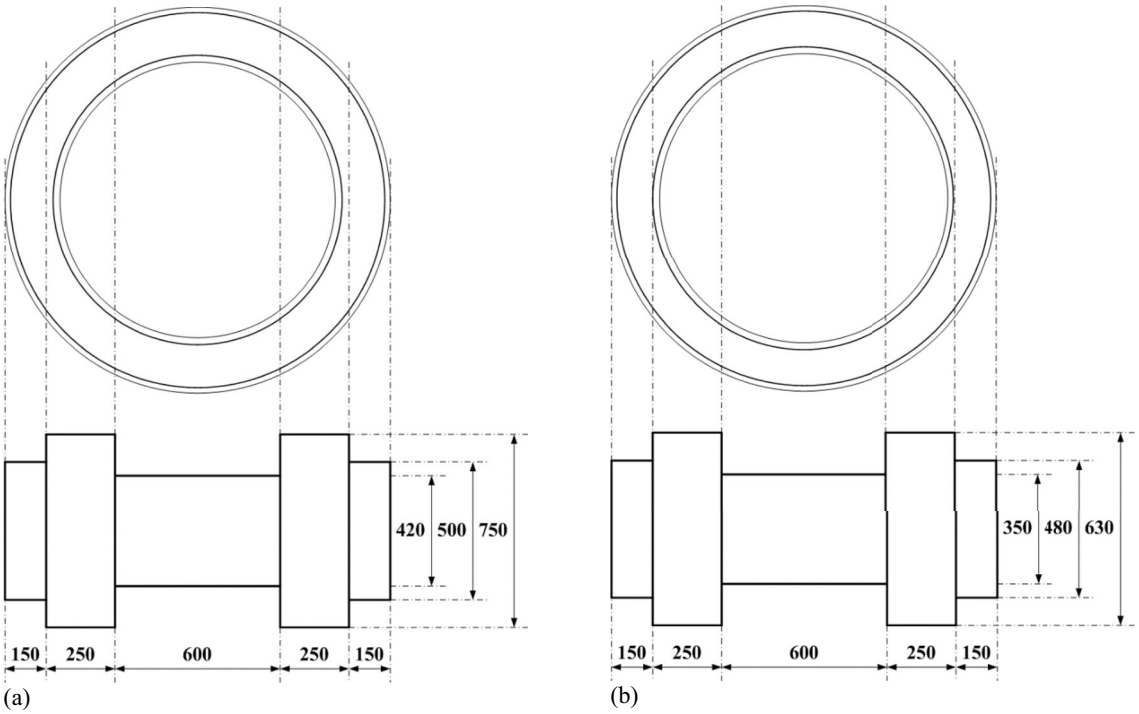

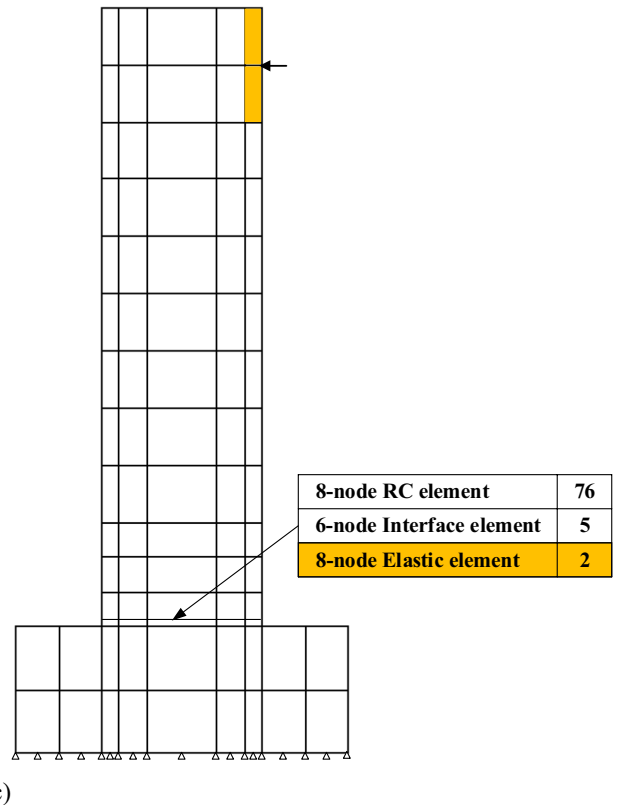

Fig. 7 Finite element model for specimen (Unit: mm): **a** Transformation of a hollow circular pier to an idealized equivalent rectangular pier (HC-D1), **b** Transformation of a hollow circular pier to an idealized equivalent rectangular pier (HC-D2) and **c** Finite element mesh for specimen

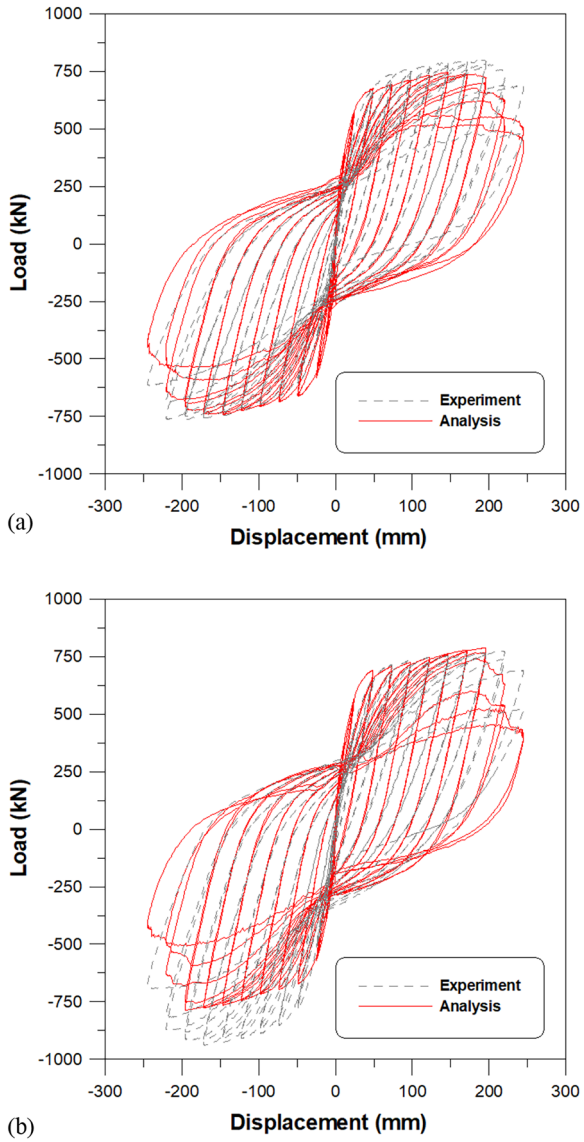

Fig. 8 Comparison of experimental and analytical results: **a** HC-D1 and **b** HC-D2

The concrete cover detached at the plastic hinge region due to repeated loading. After exhibiting significant deformation capacity, the main reinforcing bar eventually fractured due to repeated buckling and tensioning of the exposed reinforcing bars (Kim et al., 2014, 2019).

4.3 A Parametric Study of Elongation Reduction

In this study, hollow RC bridge pier specimens, illustrated in Fig. 5 of Sect. 4.1, were selected for a parametric study related to the elongation reduction of deteriorated reinforcing bars due to aging and other factors, based on varying corrosion levels.

Corrosion levels were set at 7%, 14%, 20%, and 30% according to results from previous studies (Kim, 2023). To simulate the seismic performance degradation of bridge structures due to chemical and physical factors, the deterioration model described in Sect. 2 was integrated into the validated nonlinear material model from previous studies (Kim, 2019, 2022, 2023; Kim et al., 2005, 2007, 2019). This extended model was applied to the elements corresponding to longitudinal and transverse reinforcement. The developed nonlinear deterioration model accounts for the loss of cross-sectional area due to corroded reinforcing bars, reduction in bond strength between reinforcing bars and concrete, and decrease in ductility.

Figs. 9 10 compare the analytical results with the comparable results of HC-D1 and HC-D2 from the previous section, across corrosion levels of 7%, 14%, 20%, and 30%. These figures also include comparisons based on whether the elongation of the deteriorated reinforcing bars was reduced. The results indicate that an increase in corrosion level reduces both the load-bearing capacity and energy dissipation of the hollow RC bridge piers. Additionally, the data demonstrate a direct relationship between corrosion level and the seismic performance of the hollow RC bridge piers.

Figs. 11, 12 illustrate the seismic performance evaluation of hollow RC bridge pier specimens that deteriorated due to aging and other factors by comparing changes in the damage index with drift ratios and performance levels. The results effectively simulate the behavior where damage progresses with increasing corrosion levels. These analytical results generally align with experimental observations, showing that inelastic deformation in the plastic hinge region under seismic loading leads to concrete cracking and shattering, resulting in damage or failure.

Upon examining the damage index values from the analytical results at each loading phase in Fig. 11a, which does not account for the elongation reduction of HC-D1, the following observations were made: at a drift of 0.25%, the damage index is 0.05 for the test specimen with 0% corrosion, 0.06 for the test specimen with 7% corrosion, 0.06 for the test specimen with 14% corrosion, 0.06 for the test specimen with 20% corrosion, and 0.06 for the test specimen with 30% corrosion. At a drift of 1.00%, the damage index is 0.19 for the test specimen with 0% corrosion, 0.21 for the test specimen with 7% corrosion, 0.37 for the test specimen with 14% corrosion, 0.39 for the test specimen with 20% corrosion, and 0.45 for the test specimen with 30% corrosion. At a drift of 2.00%, the damage index is 0.43 for the test specimen with 0% corrosion, 0.45 for the test specimen with 7% corrosion, 0.45 for the test specimen with 14%

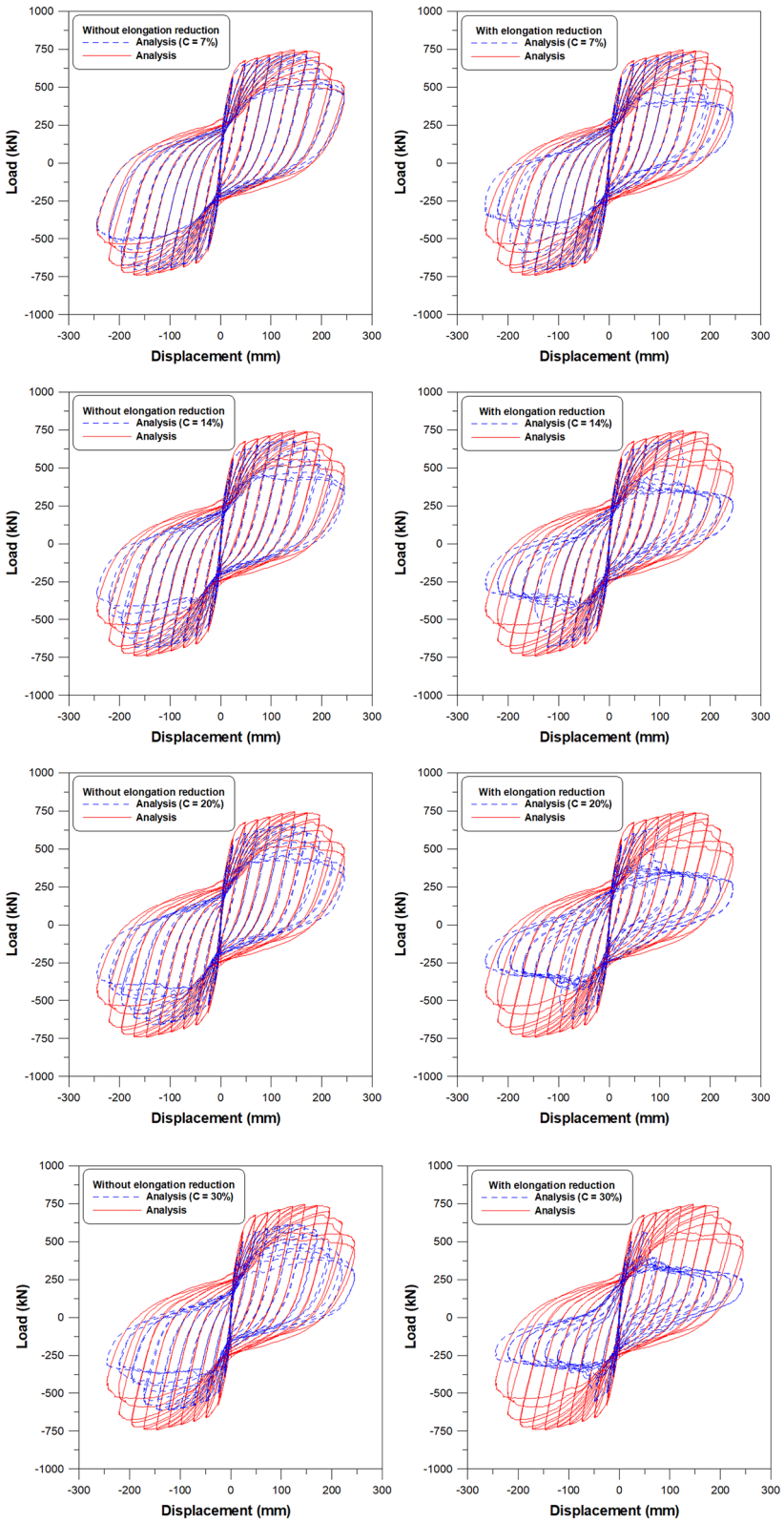

Fig. 9 Comparison of results from the analytical results for HC-D1

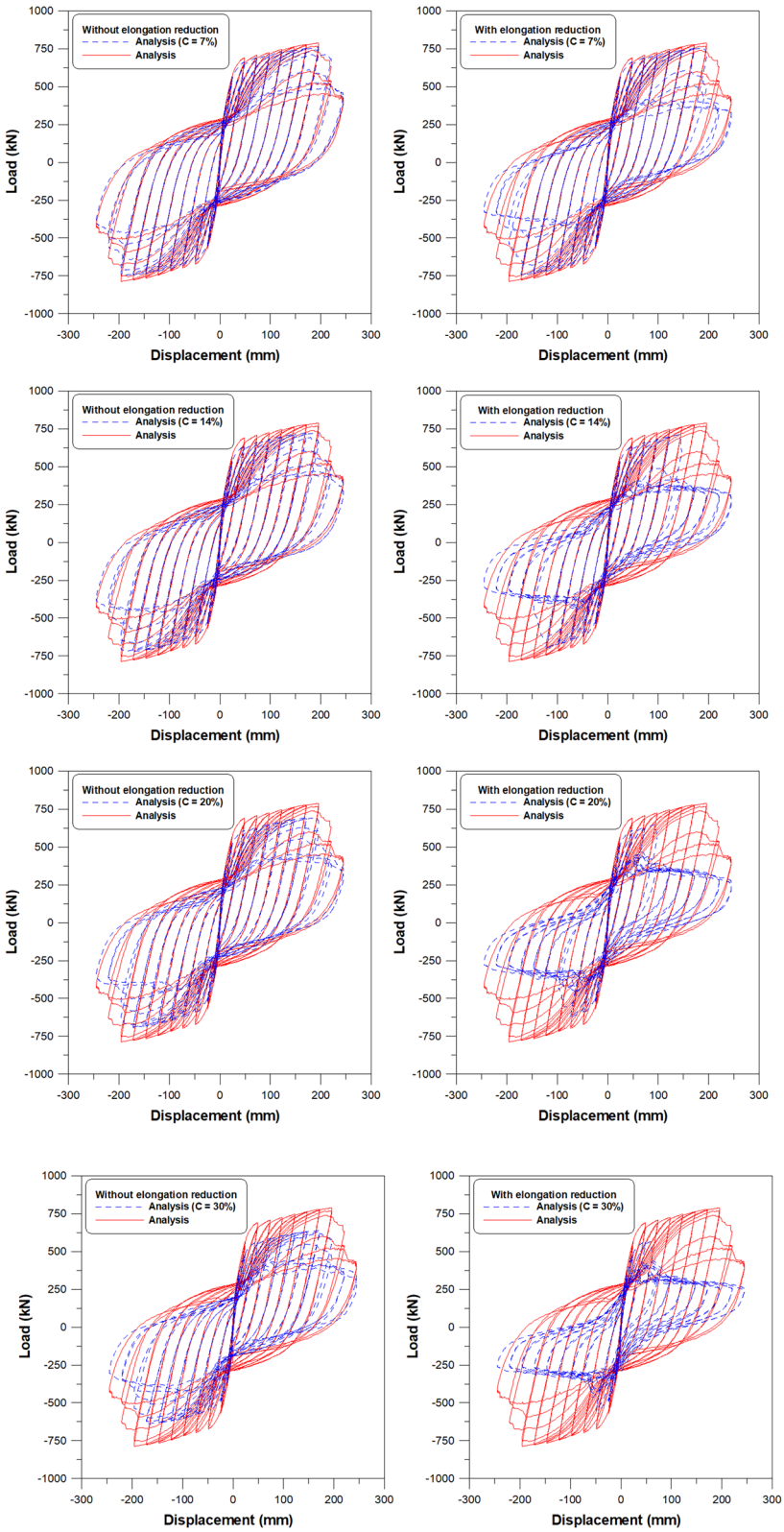

Fig. 10 Comparison of results from the analytical results for HC-D2

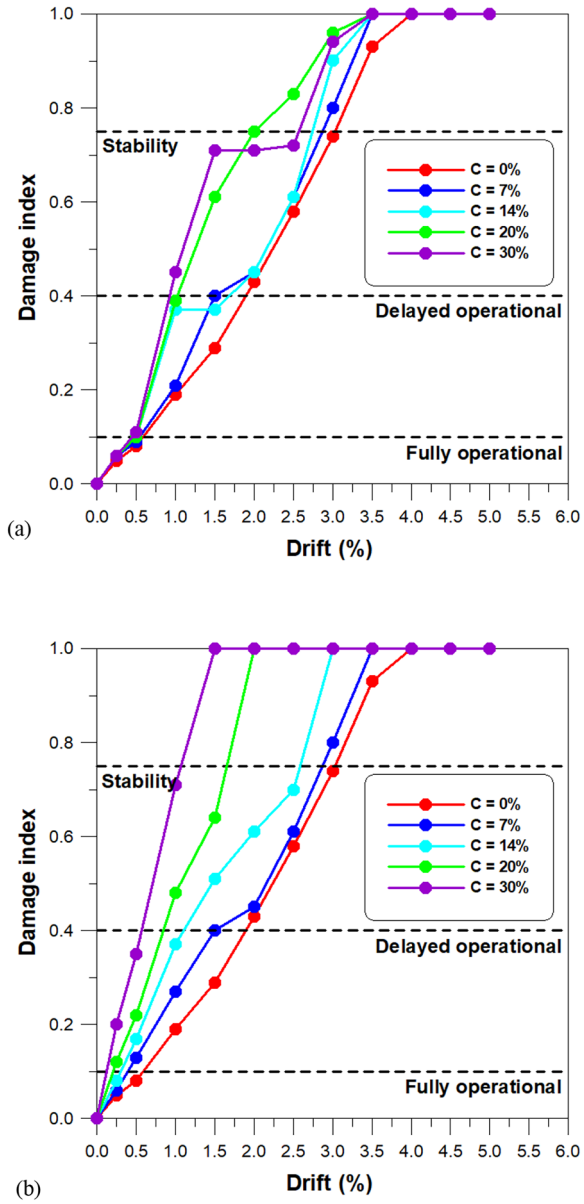

Fig. 11 Comparison of results from the analytical results for HC-D1: **a** Without elongation reduction and **b** With elongation reduction

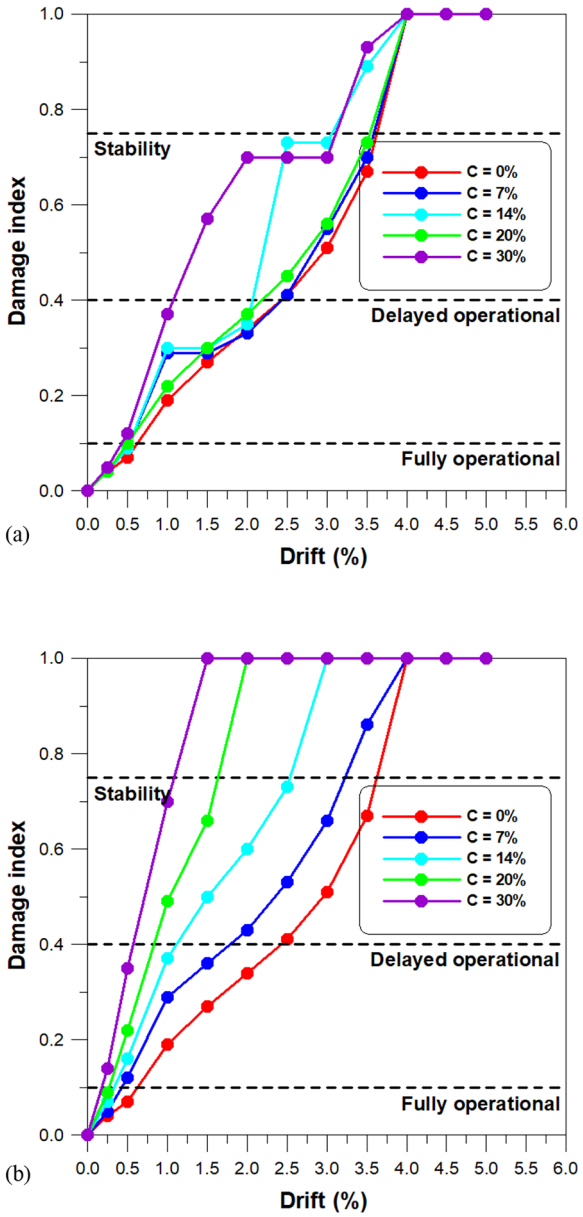

Fig. 12 Comparison of results from the analytical results for HC-D2: **a** Without elongation reduction and **b** With elongation reduction

corrosion, 0.75 for the test specimen with 20% corrosion, and 0.71 for the test specimen with 30% corrosion. At a drift of 3.00%, the damage index is 0.74 for the test specimen with 0% corrosion, 0.80 for the test specimen with 7% corrosion, 0.90 for the test specimen with 14% corrosion, 0.96 for the test specimen with 20% corrosion, and 0.94 for the test specimen with 30% corrosion. In these analytical results, which do not account for elongation reduction, a reversal phenomenon is observed in some cases, where the damage index decreases as the corrosion level increases.

Upon examining the damage index values from the analytical results at each loading phase in Fig. 11b, which considers the elongation reduction of deteriorated reinforcing bars—a factor that greatly affects seismic performance—the following observations were made: at a drift of 0.25%, the damage index is 0.05 for the test specimen with 0% corrosion, 0.06 for 7% corrosion, 0.08 for 14% corrosion, 0.12 for 20% corrosion, and 0.20 for 30% corrosion. At a drift of 1.00%, the damage index is 0.19 for 0% corrosion, 0.27 for 7% corrosion, 0.37 for 14% corrosion, 0.48 for 20% corrosion,

Table 2 Comparison of damage index results from the analytical results for HC-D1

Drift (%)	Corrosion level												
	0%	7% Without (1)	7% With (2)	(1)/(2)	14% Without (3)	14% With (4)	(3)/(4)	20% Without (5)	20% With (6)	(5)/(6)	30% Without (7)	30% With (8)	(7)/(8)
0.25	0.05	0.06	0.06	1.00	0.06	0.08	0.75	0.06	0.12	0.50	0.06	0.20	0.30
0.50	0.08	0.09	0.13	0.69	0.10	0.17	0.59	0.10	0.22	0.45	0.11	0.35	0.31
1.00	0.19	0.21	0.27	0.78	0.37	0.37	1.00	0.39	0.48	0.81	0.45	0.71	0.63
1.50	0.29	0.40	0.40	1.00	0.37	0.51	0.73	0.61	0.64	0.95	0.71	1.00	0.71
2.00	0.43	0.45	0.45	1.00	0.45	0.61	0.74	0.75	1.00	0.75	0.71	1.00	0.71
2.50	0.58	0.61	0.61	1.00	0.61	0.70	0.87	0.83	1.00	0.83	0.72	1.00	0.72
3.00	0.74	0.80	0.80	1.00	0.90	1.00	0.90	0.96	1.00	0.96	0.94	1.00	0.94
3.50	0.93	1.00	1.00	1.00	1.00	1.00	1.00	1.00	1.00	1.00	1.00	1.00	1.00
4.00	1.00	1.00	1.00	1.00	1.00	1.00	1.00	1.00	1.00	1.00	1.00	1.00	1.00
4.50	1.00	1.00	1.00	1.00	1.00	1.00	1.00	1.00	1.00	1.00	1.00	1.00	1.00
5.00	1.00	1.00	1.00	1.00	1.00	1.00	1.00	1.00	1.00	1.00	1.00	1.00	1.00

and 0.71 for 30% corrosion. At a drift of 2.00%, the damage index is 0.43 for 0% corrosion, 0.45 for 7% corrosion, 0.61 for 14% corrosion, 1.00 for 20% corrosion, and 1.00 for 30% corrosion. At a drift of 3.00%, the damage index is 0.74 for 0% corrosion, 0.80 for 7% corrosion, and 1.00 for 14%, 20%, and 30% corrosion levels. These results show that the analytical model accounting for elongation reduction does not exhibit the reversal phenomenon where the damage index decreases as the corrosion level increases. Additionally, these results effectively represent the seismic behavior in which damage progresses as the corrosion level increases.

Table 2 summarizes these results for HC-D1 and compares the ratios for cases that consider elongation reduction with those that do not.

Upon examining the damage index values from the analytical results at each loading phase in Fig. 12a, which does not consider elongation reduction for HC-D2, the following observations were made: at a drift of 0.25%, the damage index is 0.04 for specimens with corrosion levels of 0%, 7%, 14%, and 20%, 0.05 for a corrosion level of 30%. At a drift of 1.00%, the damage index is 0.19 for 0% corrosion, 0.29 for 7% corrosion, 0.30 for 14% corrosion, 0.22 for 20% corrosion, and 0.37 for 30% corrosion. At a drift of 2.00%, the damage index is 0.34 for 0% corrosion, 0.33 for 7% corrosion, 0.35 for 14% corrosion, 0.37 for 20% corrosion, and 0.70 for 30% corrosion. At a drift of 3.00%, the damage index is 0.51 for 0% corrosion, 0.55 for 7% corrosion, 0.73 for 14% corrosion, 0.56 for 20% corrosion, and 0.70 for 30% corrosion. In these analytical results, which do not consider elongation reduction, the reversal phenomenon occurs in some cases where the damage index decreases as the corrosion level increases.

In contrast, when examining the damage index values from the analytical results at each loading phase in Fig. 12b, which considers the elongation reduction of deteriorated reinforcing bars—a factor that significantly affects seismic performance—the following observations were made: at a drift of 0.25%, the damage index is 0.04 for specimens with 0% corrosion, 0.05 for 7% corrosion, 0.07 for 14% corrosion, 0.09 for 20% corrosion, and 0.14 for 30% corrosion. At a drift of 1.00%, the damage index is 0.19 for 0% corrosion, 0.29 for 7% corrosion, 0.37 for 14% corrosion, 0.49 for 20% corrosion, and 0.70 for 30% corrosion. At a drift of 2.00%, the damage index is 0.34 for 0% corrosion, 0.43 for 7% corrosion, 0.60 for 14% corrosion, 1.00 for 20% corrosion, and 1.00 for 30% corrosion. At a drift of 3.00%, the damage index is 0.51 for 0% corrosion, 0.66 for 7% corrosion, and 1.00 for 14%, 20%, and 30% corrosion levels. In these results, which account for elongation reduction, the reversal phenomenon where the damage index decreases as the corrosion level increases does not occur. Furthermore, the behavior showing damage progression as the corrosion level increases is well-represented in these analytical results.

Table 3 summarizes the results for HC-D2 and compares the ratios for cases that account for elongation reduction with those that do not.

As shown, the nonlinear analysis technique proposed in this study effectively predicts the seismic behavior of hollow RC bridge piers deteriorated due to aging and other factors, providing an accurate assessment of their ultimate strength. The proposed nonlinear analysis method was validated to properly account for key design variables, including corrosion level, yield strength and ultimate strength of the reinforcing bars, and compressive strength of the concrete. Additionally, the newly extended damage index, which incorporates both the deterioration model and elongation reduction in reinforcing bars affecting behavior, effectively evaluates seismic performance. Therefore, this extended damage index is considered a valuable tool for analytically assessing the seismic performance of hollow RC bridge piers subjected to deterioration from aging and other factors.

5 Conclusions

This study presents an analytical technique for understanding the seismic behavior and evaluating the seismic performance of hollow RC bridge piers deteriorated by aging and other factors, with a deterioration model incorporated into the validated nonlinear finite element analysis program RCAHEST for RC structures. Additionally, a damage index was extended to account for the elongation reduction in reinforcing bars and was used to conduct a reliable analytical parametric study on deteriorated hollow RC bridge pier specimens. The following conclusions were drawn:

(1) The performance degradation of hollow RC bridge piers owing to reinforcing bar corrosion and concrete detachment was accurately predicted by applying a reliable deterioration model that represents the reduction in the cross-sectional area of reinforcing bars due to corrosion, as well as the reduction in strength due to concrete cracking and cover detachment.

(2) In this study, the seismic performance of hollow RC bridge piers deteriorated due to aging and other factors was assessed using an extended damage index. This index numerically represents the extent of damage to the structure owing to drift and reflects the overall performance characteristics of the structure. The study proposes a novel seismic performance evaluation technique that can be applied to performance-based seismic design.

Table 3 Comparison of damage index results from the analytical results for HC-D2

Drift (%)	Corrosion level												
	0%	7% Without (1)	7% With (2)	(1)/(2)	14% Without (3)	14% With (4)	(3)/(4)	20% Without (5)	20% With (6)	(5)/(6)	30% Without (7)	30% With (8)	(7)/(8)
0.25	0.04	0.04	0.05	0.80	0.04	0.07	0.57	0.04	0.09	0.44	0.05	0.14	0.36
0.50	0.07	0.09	0.12	0.75	0.09	0.16	0.56	0.10	0.22	0.45	0.12	0.35	0.34
1.00	0.19	0.29	0.29	1.00	0.30	0.37	0.81	0.22	0.49	0.45	0.37	0.70	0.53
1.50	0.27	0.29	0.36	0.81	0.30	0.50	0.60	0.30	0.66	0.45	0.57	1.00	0.57
2.00	0.34	0.33	0.43	0.77	0.35	0.60	0.58	0.37	1.00	0.37	0.70	1.00	0.70
2.50	0.41	0.41	0.53	0.77	0.73	0.73	1.00	0.45	1.00	0.45	0.70	1.00	0.70
3.00	0.51	0.55	0.66	0.83	0.73	1.00	0.73	0.56	1.00	0.56	0.70	1.00	0.70
3.50	0.67	0.70	0.86	0.81	0.89	1.00	0.89	0.73	1.00	0.73	0.93	1.00	0.93
4.00	1.00	1.00	1.00	1.00	1.00	1.00	1.00	1.00	1.00	1.00	1.00	1.00	1.00
4.50	1.00	1.00	1.00	1.00	1.00	1.00	1.00	1.00	1.00	1.00	1.00	1.00	1.00
5.00	1.00	1.00	1.00	1.00	1.00	1.00	1.00	1.00	1.00	1.00	1.00	1.00	1.00

(3) The reversal phenomenon of the damage index observed in the performance phase owing to drift was reasonably addressed by incorporating elongation, a residual material property of corroded reinforcing bars obtained through regression analysis of reliable test data.
(4) The analytical seismic performance evaluation technique proposed based on a series of experimental and analytical results effectively evaluated the seismic response and performance of hollow RC bridge piers that have deteriorated due to aging and other factors. Consequently, this technique can serve as an analytical alternative to experimental seismic performance evaluations, which are limited by time and cost. Additionally, it can be used for more rational seismic design and evaluation by accounting for the level of deterioration caused by environmental factors.
(5) Precisely investigating the bond stress–slip relationship, bond strength with concrete, and elongation while considering both uniform and pitting corrosion in future research would help accurately track seismic behavior including shear-related damage, such as ductility. Future research will include more environmental factors like freeze–thaw cycles or chloride-induced corrosion and sensitivity analysis for impact of elongation reduction across a wider range of drift ratios. Also, future research will include sensitivity analysis to quantify the influence of varying these parameters such as mechanical properties on seismic response. This advancement is expected to enable the analytical evaluation of existing aging railroad facilities and provide essential data for maintenance and improvement projects.

Acknowledgements
This research was supported by a grant from R&D Program (Development of Core Technologies for Creating New Railroad Industries, PK2404B2) of the Korea Railroad Research Institute.

Author contributions
THK planed this paper, constructed the finite element model, and analyzed the experimental results and the numerical results. IHK analyzed the experimental results and the numerical results. HMS developed the finite element model. All authors read and approved the final manuscript.

Funding
This research was supported by a grant from R&D Program (Development of Core Technologies for Creating New Railroad Industries, PK2404B2) of the Korea Railroad Research Institute.

Availability of data and materials
The research data used to support the finding of this study are described and included in the article. Furthermore, some of the data used in this study are also supported by providing references as described in the article.

Declarations

Competing interests
The author declares no competing interests.

Received: 11 September 2024 Accepted: 11 January 2025
Published online: 01 May 2025

References

AASHTO (American Association of State Highway and Transportation Officials). (2012). *AASHTO LRFD bridge design specifications* (6th ed.). AASHTO.
Ahmadi, M., Kheyroddin, A., & Kioumarsi, M. (2021). Prediction models for bond strength of steel reinforcement with consideration of corrosion. *Materials Today: Proceedings, 45*, 5829–5834. https://doi.org/10.1016/j.matpr.2021.03.263
Apostolopoulos, C. A., Demis, S., & Papadakis, V. G. (2013). Chloride-induced corrosion of steel reinforcement—mechanical performance and pit depth analysis. *Construction and Building Materials, 38*, 139–146. https://doi.org/10.1016/j.conbuildmat.2012.07.087
Apostolopoulos, C. A., & Papadakis, V. G. (2008). Consequences of steel corrosion on the ductility properties of reinforcement bar. *Construction and Building Materials, 22*(12), 2316–2324. https://doi.org/10.1016/j.conbuildmat.2007.10.006
Bhargava, K., Ghosh, A. K., Mori, Y., & Ramanujam, S. (2007). Corrosion-induced bond strength degradation in reinforced concrete—analytical and empirical models. *Nuclear Engineering and Design, 237*(11), 1140–1157. https://doi.org/10.1016/j.nucengdes.2007.01.010
Biondini, F., Camnasio, E., & Palermo, A. (2014). Lifetime seismic performance of concrete bridges exposed to corrosion. *Structure and Infrastructure Engineering, 10*(7), 880–900. https://doi.org/10.1080/15732479.2012.761248
Cardone, D., Perrone, G., & Sofia, S. (2013). Experimental and numerical studies on the cyclic behavior of R/C hollow bridge piers with corroded rebars. *Earthquakes and Structures., 4*(1), 41–62. https://doi.org/10.12989/eas.2013.4.1.041
Cassese, P., De Risi, M. T., & Verderame, G. M. (2020). Seismic assessment of existing hollow circular reinforced concrete bridge piers. *Journal of Earthquake Engineering, 24*(10), 1566–1601. https://doi.org/10.1080/13632469.2018.1471430
Crespi, P., Zucca, M., Valente, M., & Longarini, N. (2022). Influence of corrosion effects on the seismic capacity of existing RC bridges. *Engineering Failure Analysis, 140*, 106546. https://doi.org/10.1016/j.engfailanal.2022.106546
El-Joukhadar, N., Dameh, F., & Pantazopoulou, S. (2023). Seismic modelling of corroded reinforced concrete columns. *Engineering Structures, 275*, 115251. https://doi.org/10.1016/j.engstruct.2022.115251
Ghosh, J., & Padgett, J. E. (2012). Impact of multiple component deterioration and exposure conditions on seismic vulnerability of concrete bridges. *Earthquakes and Structures, 3*(5), 649–673. https://doi.org/10.12989/eas.2012.3.5.649
Kim, T.-H. (2019). Analytical seismic performance assessment of hollow reinforced concrete bridge columns. *Magazine of Concrete Research, 71*(14), 719–733. https://doi.org/10.1680/jmacr.17.00463
Kim, T.-H. (2022). Seismic performance assessment of deteriorated two-span reinforced concrete bridges. *International Journal of Concrete Structures and Materials*. https://doi.org/10.1186/s40069-022-00498-9
Kim, T.-H. (2023). Analytical performance assessment of deteriorated prestressed concrete beams. *International Journal of Concrete Structures and Materials*. https://doi.org/10.1186/s40069-023-00624-1
Kim, T.-H., Kim, I.-H., Lee, J.-H., & Shin, H. M. (2019). Hollow bridge columns with triangular confining reinforcement. *Canadian Journal of Civil Engineering, 46*(6), 467–480. https://doi.org/10.1139/cjce-2018-0353
Kim, T.-H., Kim, Y.-J., Kang, H.-T., & Shin, H. M. (2007). Performance assessment of reinforced concrete bridge columns using a damage index. *Canadian Journal of Civil Engineering, 34*(7), 843–855. https://doi.org/10.1139/l07-003
Kim, T.-H., Lee, J.-H., & Shin, H. M. (2014). Performance assessment of hollow reinforced concrete bridge columns with triangular reinforcement

details. *Magazine of Concrete Research, 66*(16), 809–824. https://doi.org/10.1680/macr.13.00257
Kim, T.-H., Lee, K.-M., Chung, Y.-S., & Shin, H. M. (2005). Seismic damage assessment of reinforced concrete bridge columns. *Engineering Structures, 27*(4), 576–592. https://doi.org/10.1016/j.engstruct.2004.11.016
Kolozvari, K., Orakcal, K., & Wallace, J. W. (2018). New opensees models for simulating nonlinear flexural and coupled shear-flexural behavior of RC walls and columns. *Computers and Structures, 196*, 246–262. https://doi.org/10.1016/j.compstruc.2017.10.010
Lee, H.-S., & Cho, Y.-S. (2009). Evaluation of the mechanical properties of steel reinforcement embedded in concrete specimen as a function of the degree of reinforcement corrosion. *International Journal of Fracture, 157*, 81–88. https://doi.org/10.1007/s10704-009-9334-7
Lee, J.-H., Kim, D.-H., & Choi, J.-H. (2011). Evaluation of minimum extensibility standard requirements for steel reinforcement. *Journal of the Korea Concrete Institute, 23*(5), 559–567. https://doi.org/10.4334/JKCI.2011.23.5.559
Lee, J.-H., Kim, H.-Y., & Kwak, I. J. (2017). Behavior of rectangular hollow bridge compression section by detail of cross-tie. *Journal of the Earthquake Engineering Society of Korea, 21*(1), 21–29. https://doi.org/10.5000/EESK.2017.21.1.021
Lignola, G. P., Nardone, F., Prota, A., Luca, A. D., & Nanni, A. (2012). Analysis of RC hollow columns strengthened with GFRP. *Journal of Composites for Construction, ASCE, 15*(4), 545–556. https://doi.org/10.1061/(ASCE)CC.1943-5614.0000192
Mander, J. B., Priestley, M. J. N., & Park, R. (1988). Theoretical stress-strain model for confined concrete. *Journal of Structural Engineering, ASCE, 114*(8), 1804–1826. https://doi.org/10.1061/(ASCE)0733-9445(1988)114:8(1804)
MCT (Ministry of Construction and Transportation). (2015). *Korean Highway Bridge Design Code(Limit State Design)*. MCT.
Nepa, J., Chen, H.-P., & Alani, A. M. (2013). Analytical modelling of bond strength degradation due to reinforcement corrosion. *Key Engineering Materials, 569–570*, 1060–1067. https://doi.org/10.4028/www.scientific.net/KEM.569-570.1060
Pantazopoulou, S. J., & Papoulia, K. D. (2001). Modeling cover-cracking due to reinforcement corrosion in RC structures. *Journal of Engineering Mechanics, ASCE, 127*, 342–351. https://doi.org/10.1061/(ASCE)0733-9399(2001)127:4(342)
Rajput, A. S., & Sharma, U. K. (2018). Corroded reinforced concrete columns under simulated seismic loading. *Engineering Structures, 171*, 453–463. https://doi.org/10.1016/j.engstruct.2018.05.097
Rinaldi, Z., Carlo, F. D., Spagnuolo, S., & Meda, A. (2022). Influence of localised corrosion on the cyclic response of reinforced concrete columns. *Engineering Structures, 256*, 114037. https://doi.org/10.1016/j.engstruct.2022.114037
Stewart, M. G., & Al-Harthy, A. (2008). Pitting corrosion and structural reliability of corroding RC structures: Experimental data and probabilistic analysis. *Reliability Engineering & System Safety, 93*(3), 373–382. https://doi.org/10.1016/j.ress.2006.12.013
Sun, C.-H., & Kim, I.-H. (2009). Seismic characteristics of hollow rectangular sectional piers with reduced lateral reinforcements. *Journal of the Earthquake Engineering Society of Korea, 13*(3), 51–65. https://doi.org/10.5000/EESK.2009.13.3.051
Taylor, R. L. (2000). *FEAP – A Finite Element Analysis Program, Version 7.2 Users Manual*. University of California at Berkeley.
Toongoenthong, K., & Maekawa, K. (2005). Multi-mechanical approach to structural performance assessment of corroded RC members in shear. *Journal of Advanced Concrete Technology, 3*(1), 107–122. https://doi.org/10.3151/jact.3.107
Ueda, T., & Takewaks, K. (2007). Performance-based standard specifications for maintenance and repair of concrete structures in Japan. *Structural Engineering International, 17*, 359–366. https://doi.org/10.2749/101686607782359119
Xu, J.-G., Cai, Z.-K., & Feng, D.-C. (2021). Life-cycle seismic performance assessment of aging RC bridges considering multi-failure modes of bridge columns. *Engineering Structures, 244*, 112818.
Yeh, Y. K., Mo, Y. L., & Yang, C. Y. (2001). Seismic performance of hollow circular bridge columns. *ACI Structural Journal*. https://doi.org/10.14359/10753
Zucca, M., Reccia, E., Longarini, N., Eremeyev, V., & Crespi, P. (2023). On the structural behaviour of existing RC bridges subjected to corrosion effects: Numerical insight. *Engineering Failure Analysis, 152*, 107500. https://doi.org/10.1016/j.engfailanal.2023.107500

Publisher's Note

Tae-Hoon Kim Principal Researcher, Advanced Railroad Civil Engineering Division, Korea Railroad Research Institute, 176, Cheoldo-bangmulgwan-ro, Uiwang-si, Gyeonggi-do, 16,105, Korea.

Ick-Hyun Kim Professor, Department of Civil and Environmental Engineering, University of Ulsan, 93, Daehak-ro, Ulsan-si, Korea.

Hyun Mock Shin Emeritus Professor, School of Civil, Architectural Engineering, and Landscape Architecture, Sungkyunkwan University, 2066, Seobo-ro, Suwon-si, Gyeonggi-do, 16,419, Korea